UC Berkeley
UC Berkeley Previously Published Works

Title

Compensation-Winding-Current-Based Constant On-Time Control of Trans-Inductor Voltage Regulators (TLVRs)

Permalink

https://escholarship.org/uc/item/0p83x8vd

Journal

Proceedings of the 41st Applied Power Electronics Conference and Exposition

Authors

Zhang, Shuyu
Zhu, Yicheng
Biesterfeld, Nathan
et al.

Publication Date

2026-04-27

Peer reviewed

eScholarship.org Powered by the California Digital Library
University of California

Berkeley
UNIVERSITY OF CALIFORNIA

©2026 IEEE

Proceedings of the 41st Applied Power Electronics Conference and Exposition (APEC 2026), San Antonio, Texas, USA, 22-26 March, 2026

Compensation-Winding-Current-Based Constant On-Time Control of Trans-Inductor Voltage Regulators (TLVRs)

Shuyu Zhang
Yicheng Zhu
Nathan Biesterfeld
R. C. N. Pilawa-Podgurski

Personal use of this material is permitted. Permission from IEEE must be obtained for all other uses, in any current or future media, including reprinting/republishing this material for advertising or promotional purposes, creating new collective works, for resale or redistribution to servers or lists, or reuse of any copyrighted component of this work in other works.

Compensation-Winding-Current-Based Constant On-Time Control of Trans-Inductor Voltage Regulators (TLVRs)

Shuyu Zhang, Yicheng Zhu, Nathan Biesterfeld, and Robert C. N. Pilawa-Podgurski
Department of Electrical Engineering and Computer Sciences, University of California, Berkeley
Email: {shuyu-zhang, yczhu, biesterfeld, pilawa}@berkeley.edu

***Abstract*—This paper proposes a compensation-winding-current (i_{Lc})-based constant on-time (COT) control strategy for trans-inductor voltage regulators (TLVRs) used in data center applications. Compared with conventional current-mode COT control of TLVRs, which requires high-bandwidth current sensing for each phase, the proposed approach achieves equivalent transient performance by sensing only i_{Lc}, thereby significantly reducing the system complexity. The high-pass filter nature of i_{Lc}-based current sensing and the corresponding preservation of the high-frequency current ripple needed for COT control is derived analytically and verified through circuit simulation. The proposed control strategy is experimentally validated on a six-phase, 500 kHz, 12 V-to-1 V, 240 A TLVR prototype, demonstrating robust load regulation under a $6\mathrm{A/ns}$ load step generated by a custom on-board GaN-based load stepper.**

I. Introduction

The rapid growth of artificial intelligence requires increasingly power-hungry processors (e.g. CPUs and GPUs). As the power rating of the high-performance processors continues to increase, power converters must not only deliver excellent steady-state performance but also meet demanding transient response requirements [1], including high di/dt load steps (e.g., higher than $1\ \mathrm{A/ns}$) with minimal output voltage overshoots and undershoots [2].

Trans-inductor voltage regulators (TLVRs) [3] have been an increasingly attractive solution for data center voltage regulator modules (VRM) over the past few years [4]. Fig. 1 shows the schematic diagram of a single-secondary TLVR [5] (four phases as an example). It consists of N complementary switch pairs and an N-phase indirect-coupled inductor (ICL) [6]. Fig. 2 shows the operation waveforms in the steady state. Compared to conventional multiphase buck converters, TLVRs provide different steady-state and transient equivalent inductances, thereby improving transient performance while maintaining the same inductor current ripple to keep high efficiency [5], [7], [8]. Compared to their direct-coupled inductor (DCL)-based counterparts, the unique advantages of TLVRs include flexibility in PCB layout, simple magnetic core design, improved scalability to different phase counts, and easier control and adjustment of interphase coupling.

At present, most TLVR designs inherit the control scheme of multiphase buck converters with some minor protection and optimization for TLVRs [9]. The most prevalent control scheme is current-mode constant on-time control (CMCOT) [10]–[15]. CMCOT relies on the high-frequency inductor current ripple to close the current loop and ensure stability and

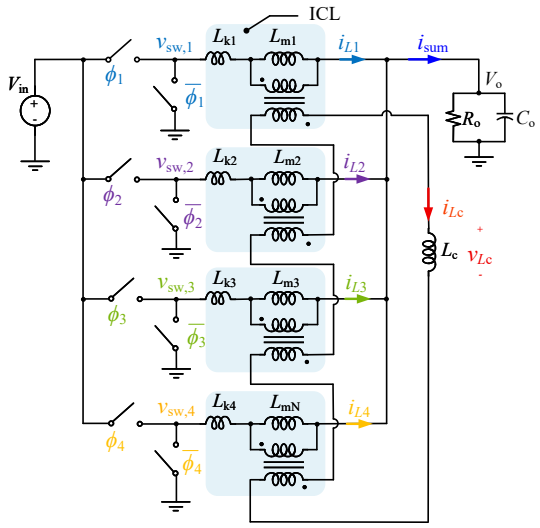


Fig. 1: Schematic diagram of a single-secondary four-phase TLVR

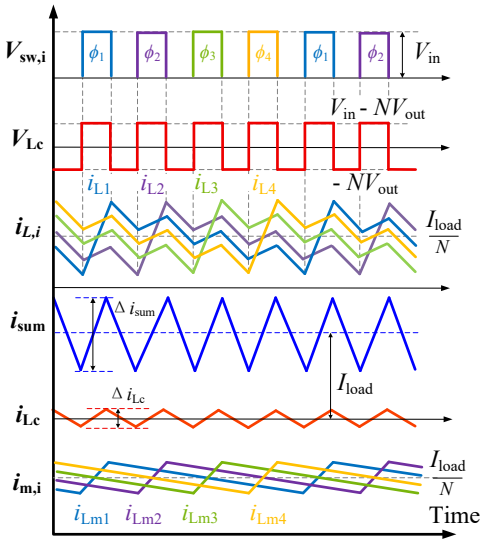
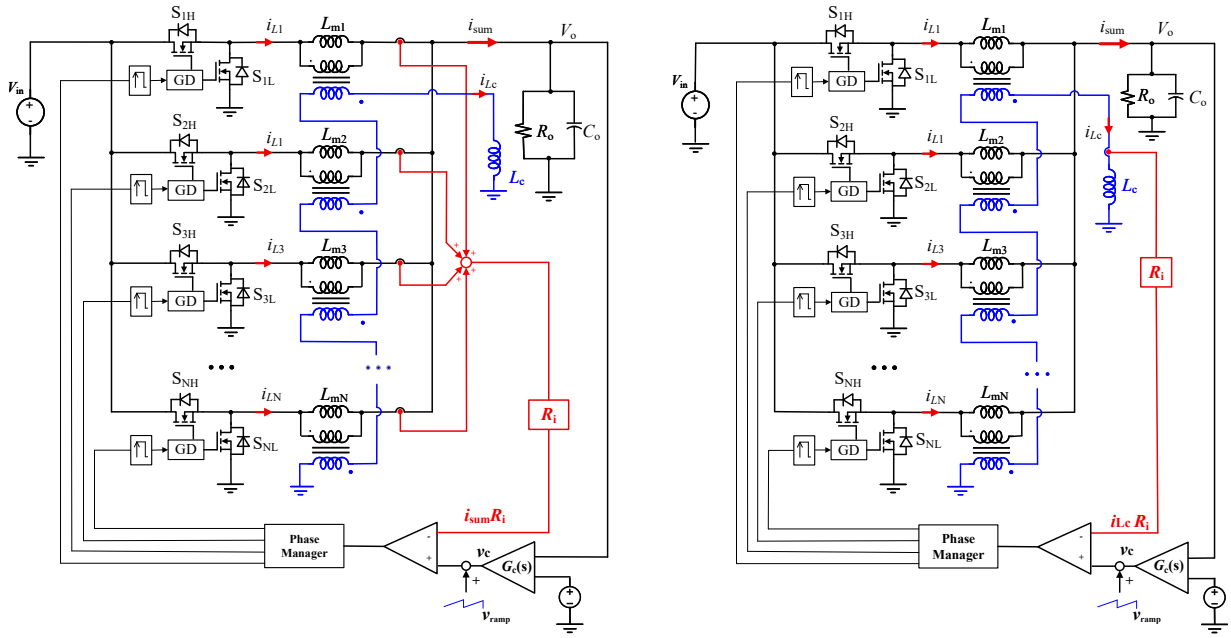


Fig. 2: Steady-state operation waveforms of the single-secondary four-phase TLVR



(a) (b)

Fig. 3: Comparison between conventional and proposed control strategies for TLVRs. (a) Conventional COT using summed inductor current (b) Proposed i_{L_c}-based COT control

.

dynamic response [16]. In a CMCOT-controlled multiphase buck converter, typically the per-phase inductor currents are sensed and sent to the controller. Within the controller, a summing circuit adds up the currents of N phases to obtain i_{sum}, which is then fed into the current loop [17].

However, implementing high-frequency inductor current sensing for VRMs, which requires high gain, high bandwidth, and usually being differential, has been proven challenging [12], [15]. The requirement for sensing is even more stringent in TLVRs. Due to interphase coupling, each phase in a TLVR carries a current ripple at a frequency of $N \times f_{\text{sw}}$, where f_{sw} denotes the per-phase switching frequency. To maintain the strength of dynamic response of TLVRs, these ripples must be preserved in both the mixed-signal PCB routing and the subsequent signal-processing circuitry. The additional bandwidth required poses a challenge for maintaining noise immunity and system reliability. With N rails of high-bandwidth sensing, the board-level complexity of TLVRs is significantly increased.

To address these challenges, this work proposes a new control scheme for TLVRs that requires the high-bandwidth sensing of only the compensation winding current (i_{L_c}). This is enabled by the fact that i_{L_c} contains the high-frequency ripple of the summed inductor currents i_{sum}—the key input for the COT current loop. In addition, i_{L_c} has no DC bias at steady state, which greatly simplifies the design of the current-sensing circuitry and allows for higher flexibility in hardware implementation. While prior works have been actively looking at methods to sense the i_{L_c} [18], the possibility of using it for dynamic response improvement has not yet been explored. This paper, for the first time, demonstrates utilizing i_{L_c} for COT control, with a successful hardware demonstration showing robust voltage regulation and excellent dynamic response.

II. Operating Principles of the Proposed i_{L_c}-based COT Control for TLVRs

A. Operation of TLVRs and the i_{L_c} dynamics

Fig. 3a shows the circuit schematic and control diagram of the conventional CMCOT control for TLVRs. A summing circuit adds up the sensed currents of all phases with a sensing gain of R_{i}. Then, the summed current signal $i_{\text{sum}}R_{\text{i}}$ is compared with a valley reference generated by a voltage regulation compensator ($G_c(s)$). Once i_{sum} falls below the valley, the switching transition is triggered and allocated in sequence to each phase by a phase manager. Then, the corresponding high-side switch is turned on for a pulse width of T_{on} [17].

We can derive the relationship between i_{L_c} and i_{sum} in Fig. 1 as (1)

$$\frac{di_{\text{sum}}}{dt} = \left[\frac{L_{\text{c}} + N(L_{\text{k}} + L_{\text{m}})}{mL_{\text{m}}}\right] \frac{di_{L_{\text{c}}}}{dt} \tag{1}$$

where m is the turns ratio of the transformer, which often equals to 1 for off-the-shelf indirect-coupled inductors. We usually adopt high coupling coefficient inductors where $L_{\text{k}} \approx 0$. For a single-secondary TLVR with $m = 1$, $\frac{di_{\text{sum}}}{dt} \approx (N + L_{\text{c}}/L_{\text{m}})\frac{di_{L_{\text{c}}}}{dt}$

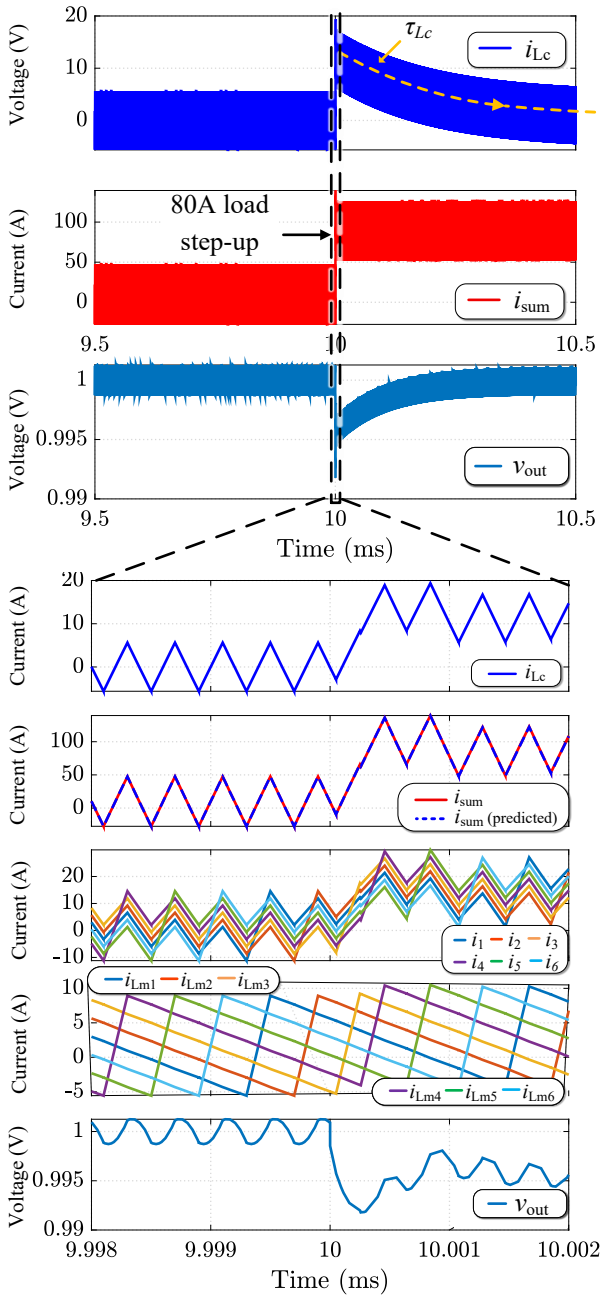


Fig. 4: PLECS simulation of summed inductor current i_{sum}, compensation winding current i_{L_c}, per phase current $i_{L_{1\sim6}}$, magnetizing current $i_{L_{m1\sim6}}$, and output voltage. $V_{\text{in}} = 12\text{V}$, $V_{\text{out}} = 1\text{V}$, $i_{\text{load}} = 10 \rightarrow 90\text{A}$. $R_{L_c} = 5\ \text{m}\Omega$, $R_{\text{ph}} = 1\ \text{m}\Omega$

The L_c winding has no voltage excitation. Therefore, in periodical steady state, i_{L_c} is an AC current, whose peak-to-peak amplitude is proportional to that of the summed inductor current i_{sum}. In Fig. 2, we can see this relationship between i_{sum} and i_{L_c}.

Whenever the i_{L_c} obtains an offset due to a sharp increase or decrease of the phase currents, such as during a load-step transient event, it naturally decays to zero. Under stringent

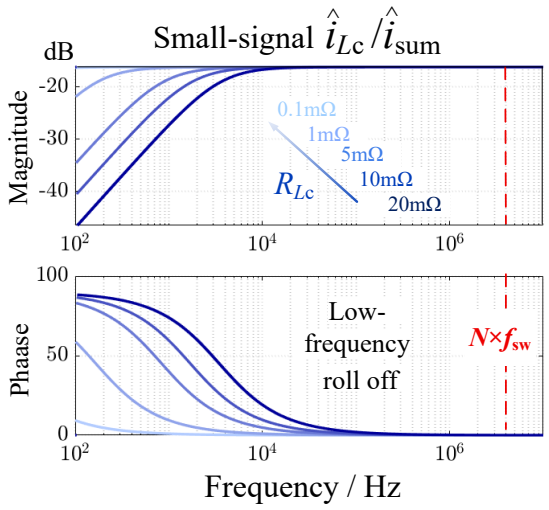


Fig. 5: PLECS simulation of the high-pass filter nature of i_{L_c} response to i_{sum}. $L_m = 150$ nH, $L_c = 100$ nH, six phase, sweeping R_{L_c} from 0.1 mΩ to 20 mΩ

output voltage regulation, the zero-input RL damping time constant of i_{L_c} is

$$\tau_{L_c} \approx \frac{NL_m/m^2 + L_c}{R_{L_c}} \tag{2}$$

where N is the phase count, R_{L_c} is the lumped resistance in the compensation winding, including the winding resistance and the PCB parasitic resistance. Fig. 4 shows the damping characteristics.

In a well-designed high-current power converter system for data center applications, the parasitic resistance is usually optimized to be very low (e.g., a few mΩ per phase) to improve efficiency. Therefore, the damping time constant τ_{L_c} is typically far longer than the response time of a typical current control loop. Fig. 5 demonstrates that the transfer function from an i_{sum} perturbation to an i_{L_c} response is a high-pass filter whose the roll-off frequency is determined by the loop parasitic resistance. As the parasitic resistance R_{L_c} increases from 0.1 mΩ to 20 mΩ, the roll-off frequency increases but remains sufficiently below the operating frequency (N times of the switching frequency in an N-phase interleaved TLVR) of the current control loop for i_{L_c} to be used in CMCOT control.

Fig. 4 presents the zoomed waveform of the summed inductor current i_{sum} and i_{L_c} during a load step. During the short timescale of load transients (on the order of μs), the change in i_{sum} is proportional to the change in i_{L_c}, enabling precise prediction of i_{sum} by sensing i_{L_c}.

B. Proposed i_{L_c}-based COT control

Section I has revealed that at the time scale of a load transient response, Δi_{L_c} contains all the ripple information of the summed inductor current, which behaves as a high-pass filter. Notably, a fast-transient current loop requires only

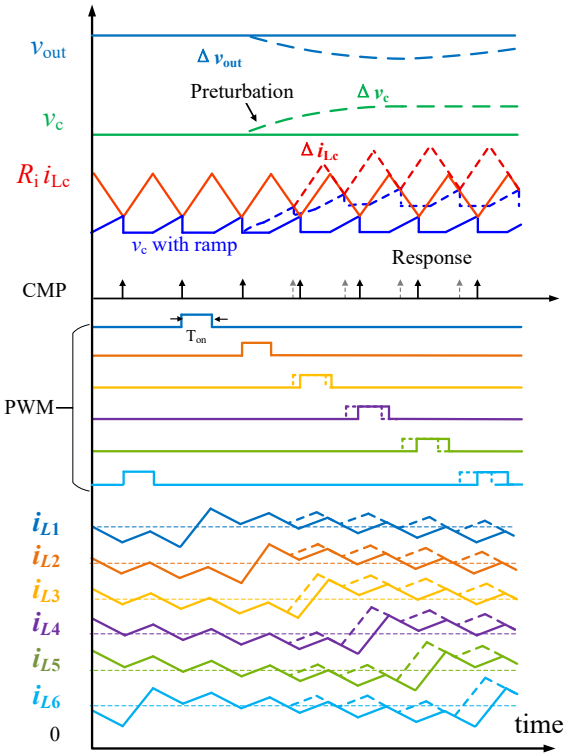


Fig. 6: Key circuit waveforms of v_c, i_{L_c}, PWM signals, per-phase current i_L, illustrating the operation principle of proposed control scheme

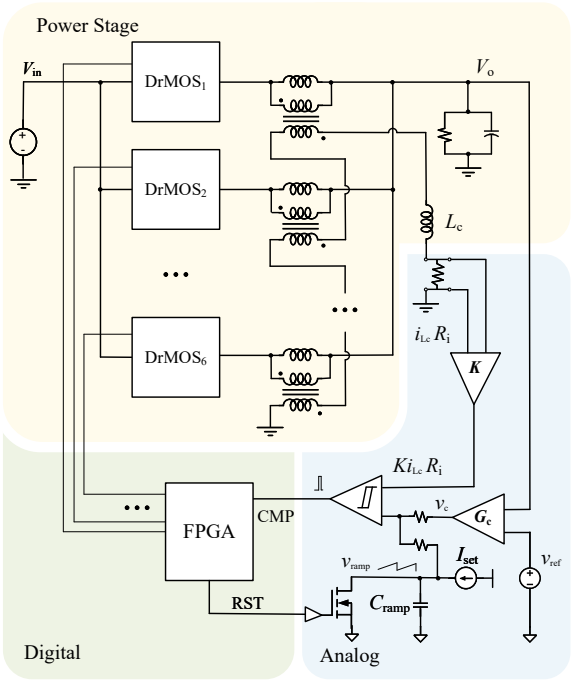


Fig. 7: Hardware implementation diagram, including the i_{L_c} sensing, the ramp generation circuit, the compensator, etc.

these high-frequency ripple components [19], [20], which is what i_{L_c} inherently possesses.

Fig. 3 highlights the difference between the proposed control strategy and the conventional multiphase COT solution. In Fig. 3b, the valley reference is compared to the sensed L_c current signal $R_i\, i_{L_c}$ instead of the summed inductor current. As is shown in Fig. 6, CMP is the comparator output, valley reference is the sum of the compensator output v_c and the external ramp v_{ramp}. Whenever the L_c current falls below the valley reference, the CMP pulse is sent to the controller, which turns the corresponding complementary switch pair on for a time of T_{on}. When there is a perturbation in v_c, as is shown in the dash lines in Fig. 6, the off time changes and i_{L_c}, as well as all the phase currents, quickly respond to the change in the valley. Although the i_{L_c} current gradually damps after many switching periods, it can be considered as "quasi-static" during the state transition due to large time constant as in Equation (2). Therefore, the voltage regulation loop adjusts v_c accordingly until the i_{L_c} decays back to zero.

C. Advantages of the proposed scheme

The key advantage of the proposed i_{L_c}-based COT scheme is that it replaces the N per-phase high-bandwidth differential current sensors with one ground-referenced high-bandwidth differential current sensor for L_c, offering lower complexity and increased flexibility in hardware implementation. High-bandwidth differential current sensing requires high speed, high common-mode rejection ratio (CMRR) amplifiers, which typically incurs significant cost. With i_{L_c}-based COT control, only per-phase DC current is required for current balancing and over-current protection, which significantly reduces the system cost and complexity. It is also worth noting that i_{L_c} is an AC current with much smaller RMS value than the pe-phase DC current, potentially reducing the sensing-induced losses and improving the system efficiency. Another benefit is that the proposed technique eliminates the need for additional analog circuitry to add up the N phase currents for obtaining i_{sum}, thereby further reducing the complexity of the controller. Moreover, the proposed i_{L_c}-based CMCOT is applicable to all TLVR-related topologies beyond multiphase buck converters. In particular, the proposed control technique is applicable to hybrid switched-capacitor converters with natural current-balancing capability, which eliminates the need for DC current sensing for active current balancing [12], [21].

III. Hardware Implementation and Experimental Validation

A 12V-to-1V regulated, 240A, 6-phase TLVR prototype is built to validate the proposed i_{L_c}-based COT control strategy. The nominal switching frequency is 500 kHz. Fig. 7 shows the diagram of the control and sensing circuitry, and Fig. 8 shows the experimental setup and the PCB top view. The dynamic load is implemented with a 12-rail, 20A per unit GaN-based load stepper with a slew rate of 6A/ns to emulate the high dynamic load characteristics of CPUs and GPUs.

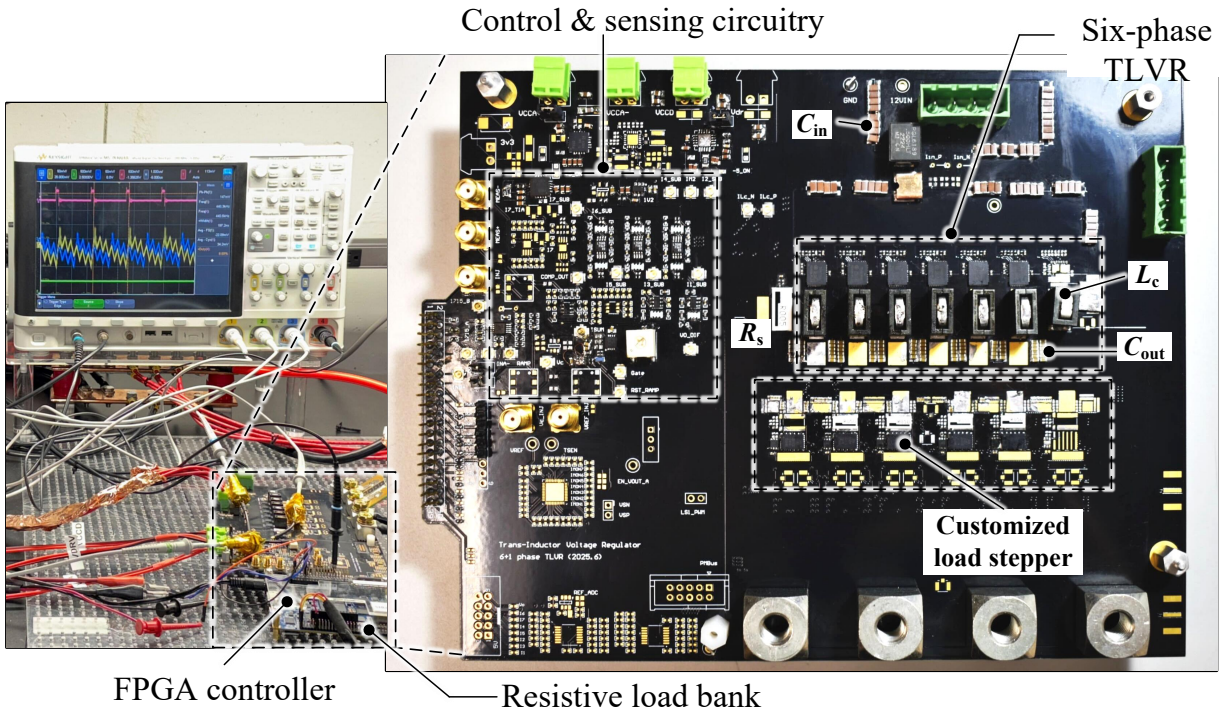


Fig. 8: Photograph of the hardware prototype for control scheme validation.

TABLE I: Component List of the Hardware Prototype

Component	Part Number	Parameters
DrMOS_{1-6}	Infineon TDA21590	16 V, 90 A
TLVR inductors	Abracon ATL-1Z110611SR15LT	$L_{\mathrm{self}} = 150$ nH, $\mathrm{DCR}_{\mathrm{pri}} = 0.125$ mΩ, $\mathrm{DCR}_{\mathrm{sec}} = 0.37$ mΩ
Inductor L_c	Coilcraft SLR7010-101KED	100 nH, DCR = 0.17 mΩ
Output capacitors C_{out}	Murata GRM21BC80G107ME15L	100 μF 4V X6S 0805* × 15
	TDK C1608X6S0G226M080AC	22 μF 4V X6S 0603* × 90
	TDK C1005X6S0G475M050BC	4.7 μF 4V X6S 0402* × 50
i_{L_c} sensing resistor	Ohmite FC4L110R005FER	5 mΩ, 1%, 5W
Load stepper resistor	Ohmite FC4L64R050FER	50 mΩ, 1%, 2W
Load stepper GaNFET	Nextperia GANE3R9-150QBA	150 V, 3.9 mΩ

* The capacitance listed is nominal value before DC derating.

Table I shows the component selection of this prototype. The power stage of this prototype uses DrMOS from Infineon. It should be noted that the current sense output of the DrMOS is used exclusively for probing and validating the current waveforms and it is not used in i_{L_c}-based CMCOT control. As is described in Section II, only i_{L_c} is fed into the control loop.

The sensing circuitry for i_{L_c} can be implemented in multiple ways, including sensing resistor [12], DCR sensing of L_c, SenseFET, etc [18]. When sensing resistors are used, the additional loss is much lower than per phase current sensing because i_{L_c} has a much lower RMS value due to its zero DC bias. In this prototype, a sensing resistor is used for validating the concept, but other lossless methods, such as DCR sensing, are also feasible.

Fig. 9 shows the experimental waveform of the transient dynamics of i_{L_c}, which aligns well with the simulation waveforms in Fig. 4. The right-hand-side figure shows zoomed-in waveforms during a load step-up transient, which clearly shows that the i_{L_c} responses with the change of the compensator output v_c, as described in Fig. 6.

Fig. 10 and Fig. 11 show the load step-up and step-down transient responses of the proposed i_{L_c}-based control strategy. The output current quickly responds to I_{load} within a few T_{on} cycles.

IV. Conclusions

This work presents a compensation-winding-current-based constant on-time (i_{Lc}-based COT) control strategy for TLVRs, with the intrinsic high-frequency AC ripple in i_{Lc} as the high-bandwidth feedback signal for the current control loop. The high-pass filtering nature from i_{sum} to i_{L_c} is derived and

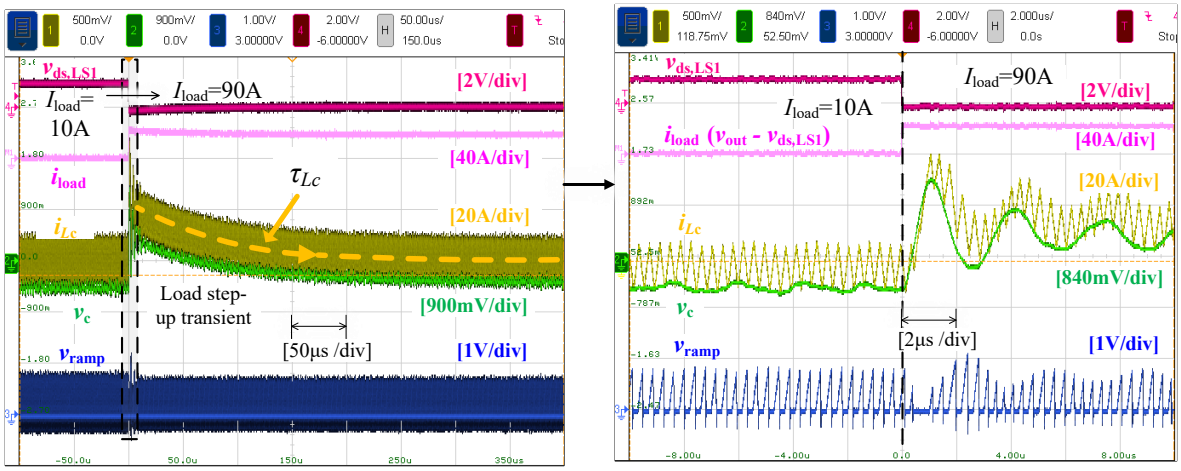


Fig. 9: Key operation waveform of proposed control strategy. i_{L_c} damping with time constant τ_{L_c} (left); zoomed-in waveform of i_{L_c}, compensator output v_c, and ramp compensation v_{ramp} during a 10 A $\rightarrow$ 90 A load step-up transient.

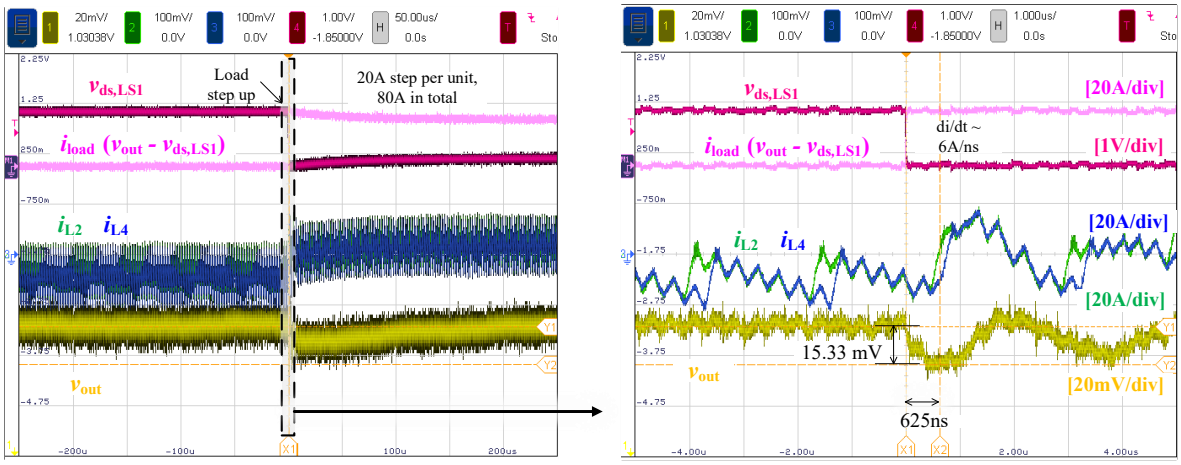


Fig. 10: Load step-up transient waveforms. 12V-to-1V, I_{load} = 10 A $\rightarrow$ 90 A. Current loop responses in 625 ns, output voltage undershoot 15.33 mV.

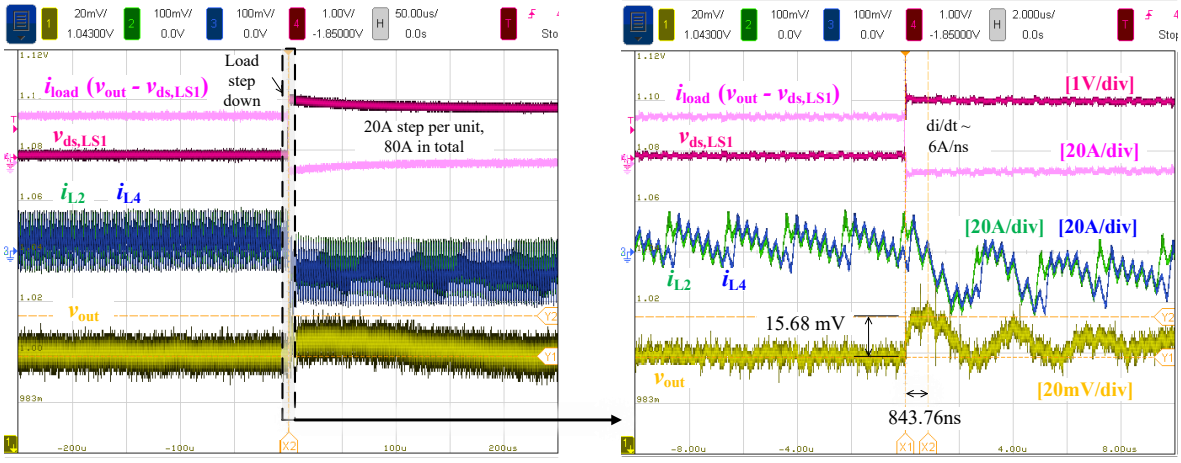


Fig. 11: Load step-down transient waveforms. 12V-to-1V, I_{load} = 90 A $\rightarrow$ 10 A. Current loop responses in 844 ns, output voltage overshoot 15.68 mV.

verified. Based on this finding, the proposed control architecture replaces N high-bandwidth per-phase current sensors with one ground-referenced high-bandwidth i_{Lc} sensor. This significantly simplifies the system complexity and eliminates the need for inductor current summation. The concept is broadly applicable to TLVR-related topologies, offering a path toward high-performance, cost-effective VRM designs. A six-phase, 12 V-to-1 V, 240 A TLVR prototype was constructed to validate the proposed control technique. Under $6\,\mathrm{A/ns}$, 80 A load steps generated by a custom GaN-based load stepper, the converter achieves current response within a few T_{on} cycles and maintains tight output-voltage regulation. The demonstrated performance shows that the proposed method retains the advantages of COT control—fast response and improved stability—while relieving the sensing and routing bottlenecks that can constrain VRM scalability.

V. Acknowledgements

The authors would like to gratefully acknowledge the Berkeley Power and Energy Center for the financial support of this project and Nexperia for providing the GaN HEMT samples for the load stepper. Author Shuyu Zhang also would like to acknowledge Yijie Qian, Southeast University, and Qi Zhou, University of Macau, for helpful discussions related to hardware design.

References

[1] Y. Chen, K. Shi, M. Chen, and D. Xu, "Data center power supply systems: From grid edge to point-of-load," *IEEE Journal of Emerging and Selected Topics in Power Electronics*, vol. 11, no. 3, pp. 2441–2456, 2023.

[2] K. Yao, Y. Ren, and F. Lee, "Critical bandwidth for the load transient response of voltage regulator modules," *IEEE Transactions on Power Electronics*, vol. 19, no. 6, pp. 1454–1461, 2004.

[3] M. Xu, F. C. Lee, and Y. Ying, "Coupled-inductor multi-phase buck converters," Patent US7 791 321B2, Sep. 7, 2010, u.S. Patent. [Online]. Available: https://patents.google.com/patent/US7791321B2

[4] "Fast multi-phase trans-inductor voltage regulator," Technical Disclosure Commons, May 2019, accessed: Aug. 2025. [Online]. Available: https://www.tdcommons.org/dpubs_series/2194.

[5] H. Shao, T. Zhao, D. Fu, D. Huang, and J. Zhou, "Analytic model and design procedure of the single-secondary trans-inductor voltage regulator," in *2021 IEEE Energy Conversion Congress and Exposition (ECCE)*, 2021, pp. 2005–2010.

[6] F. Zhu, "Investigation of multiphase coupled inductor topologies for point-of-load applications," Ph.D. dissertation, Virginia Tech, Blacksburg, VA, USA, 2023.

[7] X. Lou, F. Zhu, Z. Li, Q. Li, and F. C. Lee, "Single-stage 48 v/1.8 v coupled-transformer voltage regulator (ctvr)," in *2023 IEEE Energy Conversion Congress and Exposition (ECCE)*, 2023, pp. 2333–2339.

[8] X. Lou and Q. Li, "Single-stage 48 v/1.8 v converter with a novel integrated magnetics and 1000 w/in3 power density," *IEEE Transactions on Industrial Electronics*, vol. 71, no. 7, pp. 6601–6611, 2024.

[9] Y. Zhou, D. Clavette, J. A. Ejury, P. Kasturi, and K. Kshirsagar, "Trans-inductance multi-phase power converters and control," U.S. Patent US 11,876,445 B2, Jan. 16, 2024.

[10] N. Zhang, C. Zhan, G. Ye, C. Chen, X. Li, and J. Yi, "Analysis of multi-phase trans-inductor voltage regulator with fast transient response for large load current applications," in *2021 IEEE International Symposium on Circuits and Systems (ISCAS)*, 2021, pp. 1–5.

[11] C. Li, L. Wang, M. Fu, and H. Wang, "Small-signal modeling of multi-phase trans-inductor voltage regulator modules in datacenter applications," in *2024 IEEE Applied Power Electronics Conference and Exposition (APEC)*, 2024, pp. 633–638.

[12] L. Wang, C. Li, J. Liang, W. T. Ng, and H. Wang, "Analysis and design of ultrafast series capacitor trans-inductor voltage regulator with constant on-time control," *IEEE Transactions on Power Electronics*, vol. 40, no. 6, pp. 8315–8327, 2025.

[13] A. M. Naradhipa and Q. Li, "Multiphase lateral flux indirect coupled inductor for vertical power delivery voltage regulator module," in *2025 IEEE Applied Power Electronics Conference and Exposition (APEC)*, 2025, pp. 498–504.

[14] H. Zeng, J. Lee, R. Lai, and H. Shao, "Constant-on-time control for zero-bias trans-inductor voltage regulators," in *2025 IEEE Applied Power Electronics Conference and Exposition (APEC)*, 2025, pp. 2138–2142.

[15] C. Li, L. Wang, G. Zheng, M. Fu, and H. Wang, "Small-signal modeling and loop analysis of ultrafast series capacitor trans-inductor voltage regulator with constant on-time control," *IEEE Transactions on Power Electronics*, vol. 40, no. 2, pp. 3262–3274, 2025.

[16] Y. Qian, Y. Gao, W. Shu, L. Li, S. Xu, and W. Sun, "An ultra-fast control strategy and pre-current-balancing measures prepared for rapid transients in constant on-time controllers," in *2025 IEEE Applied Power Electronics Conference and Exposition (APEC)*, 2025, pp. 524–529.

[17] Monolithic Power Systems (MPS), "MP2965 dual-loop, digital, multi-phase controller with pmbus interface," Datasheet, 2025, accessed: Aug. 2025. [Online]. Available: https://www.monolithicpower.com/en/mp2965.html

[18] X. Chen, O. Jong, Y. Liu, J. Zhang, and M. F. Hartman, "Trans-inductor voltage regulator current sensing techniques," Patent US12 278 551B2, Apr. 15, 2025, u.S. Patent. [Online]. Available: https://patents.google.com/patent/US12278551B2

[19] S. Tian, F. C. Lee, Q. Li, and Y. Yan, "Unified equivalent circuit model and optimal design of v^2 controlled buck converters," *IEEE Transactions on Power Electronics*, vol. 31, no. 2, pp. 1734–1744, 2016.

[20] X. Lou, Q. Li, F. C. Lee, and M. H. Ahmed, "Modeling and analysis of current mode and v2 controls with adaptive voltage positioning (avp) design," in *2021 IEEE Applied Power Electronics Conference and Exposition (APEC)*, 2021, pp. 2549–2555.

[21] S. Zhang, Y. Zhu, and R. C. N. Pilawa-Podgurski, "Analysis and implementation of a series-capacitor zero-bias trans-inductor voltage regulator," in *2026 IEEE Applied Power Electronics Conference and Exposition (APEC)*, 2026.